

The (100) silicon—silicon dioxide interface.

II. The Si $L_{2,3}VV$ Auger lines

T. Kunjunny and D. K. Ferry

Colorado State University, Fort Collins, Colorado 80523

(Received 12 December 1980)

The electronic state, calculated by a slab semiempirical tight-binding method, is utilized to calculate the Si $L_{2,3}VV$ Auger transition line shapes. These calculations are carried out for (a) the free Si(100) surface, (b) the 2×1 reconstructed surface, (c) the oxygen chemisorbed surface (for both atomic and molecular oxygen), and (d) the interface between a thin oxide and Si. New states which are typical of the Si—O bonds appear as characteristic peaks corresponding to these states in the Auger spectra. These lie between the positions of the Si peak in the bulk Si and SiO₂ and correspond to previously observed experimental peaks. From comparison with the available experimental data, it appears that the initial oxidation is by atomic oxygen rather than by molecular oxygen.

I. INTRODUCTION

In recent years there has been considerable interest in the theoretical calculation of Auger lines. Several researchers¹⁻⁹ have examined the valence-band Auger line shapes for Si (i.e., $L_{2,3}VV$ and $L_1L_{2,3}V$ transitions). Houston *et al.*⁴ compared experimental results for bulk Si with the theoretical calculations of Feibelman and McGuire.¹ They extracted the transition density of states and found that the line shapes for the two transitions differ, indicating the importance of matrix element and band convolution effects. The $L_1L_{2,3}V$ line shape closely resembles the results of other measurements of the Si valence density of states, but the $L_{2,3}VV$ line showed a strong emphasis for contributions from p -like states, as opposed to the sp^3 hybrids composing the valence band.

The matrix elements for the Auger transition⁸ involve the Coulomb potential connecting initial and final states, which are represented by a core wave function and an appropriate continuum wave function identical in form to a low-energy-electron-diffraction wave function. By expanding the potentials in terms of the vector separation of ion cores \vec{R} , the Auger matrix element M is found to vary as R^{-3} . Therefore, the probability of interatomic (transitions involving two distinct atoms) Auger processes falls off very rapidly with the separation of the cores. Hence the Auger line is characteristic of a local density of filled states at the atom on which the original core hole was

created.

Following the work of Houston *et al.*, Feibelman *et al.*³ and Feibelman and McGuire¹ gave a detailed treatment of theoretical Auger lines, emphasizing and simplifying the importance of matrix element effects. Jennison² extended this theory further and showed that the partial density of states obtained from the band structure must be properly normalized for the local basis function used to calculate the atomiclike Auger matrix elements. In the present work, the Feibelman-McGuire¹ theory of Auger line shapes will be followed, which in simplified terms is a weighted average of the self-folds of ss -, sp -, and pp -type configurations. The Auger electron energy distribution $N(E)$ in the simplified form is given by

$$N(E) = W_{pp}(\rho_p \otimes \rho_p) + W_{sp}(\rho_s \otimes \rho_p) + W_{ss}(\rho_s \otimes \rho_s), \quad (1)$$

where the convolution is defined by

$$f \otimes g = \int dw f(E-w)g(w), \quad (2)$$

and the entire line is shifted by the core-state energy. Here, W_{pp} , W_{sp} , and W_{ss} are the relevant matrix elements obtained empirically for the $L_{2,3}VV$ lines in bulk Si by a set of values best fitting the experimental results of Houston *et al.*⁴

Since the Auger electron emission frequently involves valence electrons and always involves the binding energies of the core levels, the line shape as well as the most probable energy is strongly influ-

enced by the chemical environment. If strong (e.g., ionic) chemical bonding of two or more atoms occurs, the core electron levels may shift several electron volts. In ionic bonding, electron levels of electronegative elements are shifted to lower binding energies, and those electropositive elements are shifted to the higher binding energies due to the net charge transfer. A similar shift in Auger electron kinetic energy is observed between the Si *LVV* line¹⁰ in bulk silicon (90.3 eV) and in silicon dioxide (74.2 eV). When the electron density of states in the valence band is altered by the chemical environment, a change in shape is observed for the Auger peak due to transitions involving valence electrons.

For surface or interface studies, the Si *LVV* Auger line is calculated from the layer density of states (LDOS) simply as linear combinations of the self-folds of the *s*- and *p*-like local density of states on each layer of Si atoms near the surface. A weighted average of the Auger lines from different layers below the surface, in accordance with the electron escape depth, gives rise to an effective Auger line shape which is equivalent to the experimentally observed line. Detailed treatment of the electron escape-depth effects have been discussed by Tareg and Wehner⁹ and others.^{11,12} If $N(E, h)$ is the Auger electron energy distribution at a depth h , the effective Auger line shape $N(E)$ can be obtained as

$$N(E) = \sum_i N(E, h_i) e^{-h_i/\lambda},$$

where λ is the mean escape depth of Auger electrons. A value of $\lambda = 4.5 \text{ \AA}$ is used in the case of the Si *LVV* line.¹⁰

In a previous paper,¹³ hereafter referred to as paper I, calculations were carried out for the band structure and LDOS for bulk Si, the free (100) surface (both ideal and 2×1 reconstructed), the chemisorbed surface (both atomic and molecular oxygen), and the Si-SiO₂ interface. These results are used here to calculate the relevant Si *LVV* Auger transitions.

In addition to the Auger electron escape-depth effects, there are other mechanisms involved which affect the characteristics of the Auger line, such as ion knock-on broadening, the effects of sputtering, temperature effects, plasma effects, etc. These effects are not specifically considered in the line-shape calculations but are partially included by smoothing the line with a Gaussian window of suitable width.

II. CALCULATED RESULTS

The calculated Si *LVV* line shape is compared with experimental data obtained by Houston *et al.*⁴ and to the theoretical line calculated by Jennison² in Fig. 1. The calculated line is positioned so that the peak appears at 90 eV, as observed experimentally. In all following calculations, the theoretical Auger lines will be positioned with reference to this bulk Auger line. There is an apparent shift in the peak position for Jennison's curve compared to the experimental line. The overall agreement of this calculated line with the experimental curve is good, and the fit is closer to the experimental data than the earlier theoretical curve. The differences are mainly at the shoulder of the line. Jennison's curve appears narrower than the experimental line. The better fit with experiment is achieved by optimizing the Auger matrix elements for the *ss*-, *sp*-, and *pp*-type contributions of the self-folds of the density of states (DOS) instead of calculating the matrix elements from first principles. The relative values of the matrix elements used in the calculation are $ss/pp = 0.007$ and $sp/pp = 0.22$. In all subsequent calculations of the Si *LVV* Auger line, these values of the matrix elements will be used.

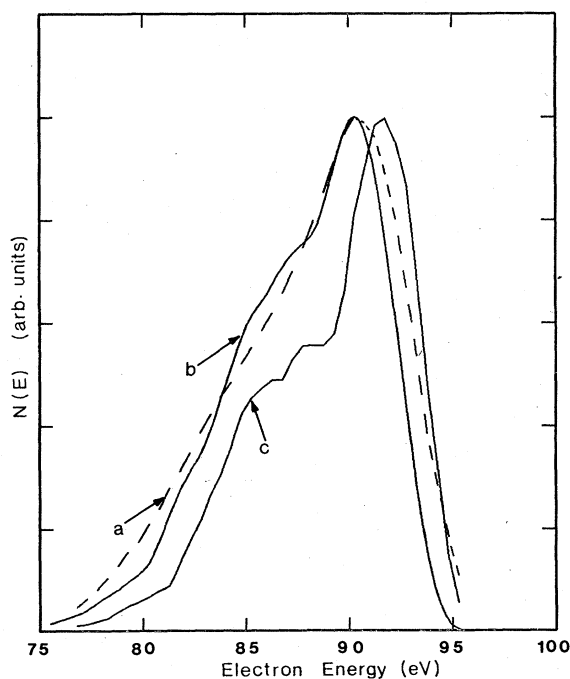


FIG. 1. Comparison of Si *LVV* Auger line shapes with experimental data: *a*—experimental data, *b*—calculated Auger line, and *c*—theoretical curve by Jennison (Ref. 2).

The ideal Si(100) L_{VV} Auger line shape is calculated from the layer density of states and shown in Fig. 2. The bulk Auger line peak is taken as the reference at an electron energy of 90 eV. The effect of the dangling-bond and bridge-bond states, which are predominantly centered at the high-energy side of the DOS near the valence-band maximum, is to shift the Auger peak to a higher energy. Since the DOS quickly relaxes to the bulk value within a few layers from the surface, the Auger lines also show the same trend, as shown in Fig. 2. The Auger lines corresponding to different layers are arbitrarily normalized and plotted here. The effective Auger line, equivalent to one experimentally observed while probing the surface, is obtained by a weighted sum of $N(E)$ contributions from different layers. The peak position for the ideal surface appears shifted by 1 eV. It is evident from these curves that the Auger contribution for the first two layers differs from the bulk contribution. For an electron escape depth of 4.5 Å and a layer depth of 1.355 Å, as is the case for the Si(100) surface, the weight of the first layer is $\sim 33\%$ while for the second layer it is $\sim 25\%$. This means that the effective line features are predominantly (nearly

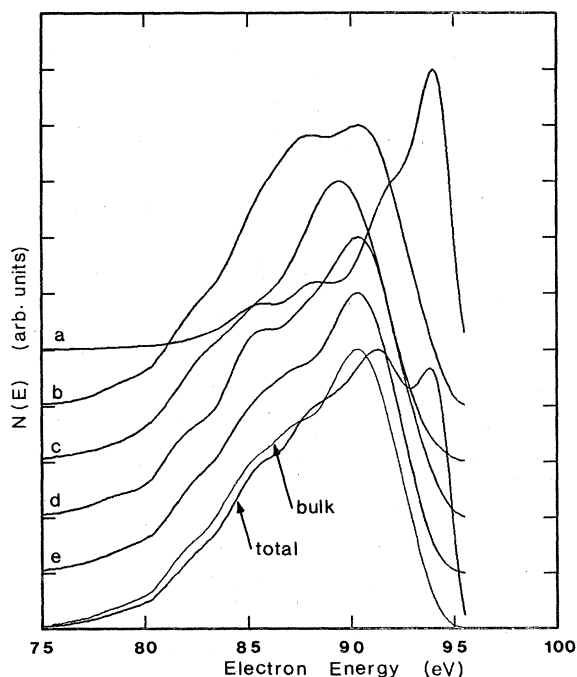


FIG. 2. Si L_{VV} Auger lines for the first five layers of Si(100) ideal surface. The effective Auger line (total) along with the bulk line are also shown. (All curves are smoothed by 1 eV.)

60%) determined by the Auger contributions of the first two layers. At this point we do not try to compare the results with experimental data, mainly since the Si(100) ideal surface is only a theoretical simplification and close agreement with experiment is not expected.

The silicon $L_{2,3}VV$ Auger lines for the reconstructed Si(100) surface are calculated from the DOS data. Since the 2×1 reconstructed surface unit cell contains two atoms, the Auger line corresponding to each layer is the sum of the Auger line from each atom in the surface unit cell. Calculated Auger line shapes for bulk Si and the Si(100) ideal and 2×1 reconstructed surfaces are shown in Fig. 3. The prominent peaks are marked A, B, C, D, where C corresponds to the main peak. The peak D is due to localized states near the valence-band maximum (VBM), and is more prominent for the case of the reconstructed surface; it is even stronger than the main peak C. This means that the dangling-bond states are overestimated. The same conclusion can be reached when the LDOS for the reconstructed surface is compared with the results from pseudopotential calculations. The peaks A (85.5 eV) and B (88.0 eV) appear in both ideal and reconstructed surfaces at approximately the same energy level. Considering the agreement of the

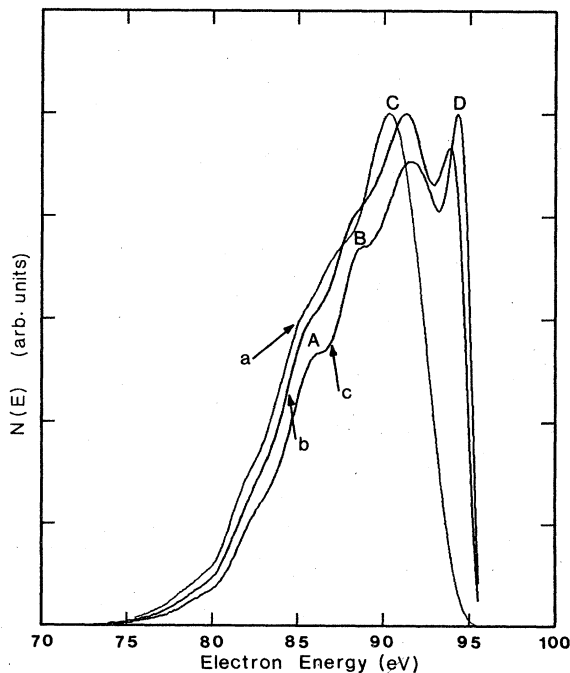


FIG. 3. Comparison of the Si L_{VV} Auger line shapes; a—bulk, b—ideal surface, and c—reconstructed surface.

DOS calculations with experimental and other theoretical results, careful measurements of the Auger lines could reveal the presence of these peaks.

The Auger line shapes calculated for the Si L_{VV} transition with atomic oxygen chemisorbed are shown in Fig. 4 for the first five silicon layers along with the effective Auger line. The absence of the dangling-bond states removes the high-energy satellite peak seen earlier for the free surface. In this figure, the first-layer Auger lines show new peaks around 70 eV. The main peak is shifted to the lower-energy direction. This is due to the fact that the center of the LDOS is shifted to lower energy by the presence of the oxygen layer. The DOS around -3 eV is greatly reduced by oxidation of the first Si layer. The effect of this on the Auger line shape is pronounced due to the fact that these are predominantly p -like states.

The calculated Auger line shapes were referenced to the Si bulk line, as mentioned above. However, it is known that the core level (Si $2p$) shifts depending on the environment. Different experimental measurements show core-level shifts of the Si $2p$ to be between 3.2 and 4.7 eV in going from Si to SiO₂.¹⁴ This large variation could be interpreted in terms of charging by x radiation rather than as a

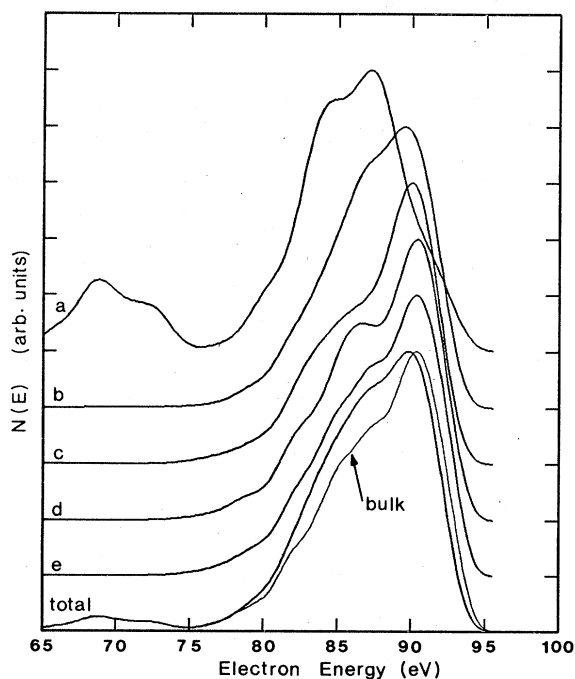


FIG. 4. The Si L_{VV} Auger lines for the first five Si layers for chemisorbed oxygen (atomic) on Si(100) ideal surface (refer to text).

chemical state change. A value of 3.2 eV is taken here as a true chemical shift, and for Si atoms which are bonded to the surface oxygen atoms, a chemical shift of only ~ 1.6 eV is used. This means the first Si-layer Auger line peak position has to be corrected accordingly. An effective Auger line is then calculated with the weighted contributions from each layer and the outer Si-layer line shifted to high energy by 1.6 eV. The results of these calculations are shown in Fig. 5. The core-level-corrected effective Auger line appears narrower than the unshifted line. Also, the peak at 68.5 eV shifts to 70 eV for the corrected effective line.

The Auger lines calculated for the various layers, with an oxygen molecule chemisorbed to the surface are shown in Fig. 6. Here, the O₂ molecule sits between the two Si dangling bonds, as discussed in paper I. The Auger line corresponding to the first Si layer shows various fine structure. There is a peak centered around 71 eV which is rather broad when compared to the similar peak in atomic chemisorption. There are also small peaks at 85, 92, and 94.5 eV, while the major peak is at ~ 90 eV as in the bulk line. The overall Auger line for the molecular chemisorbed surface seems to

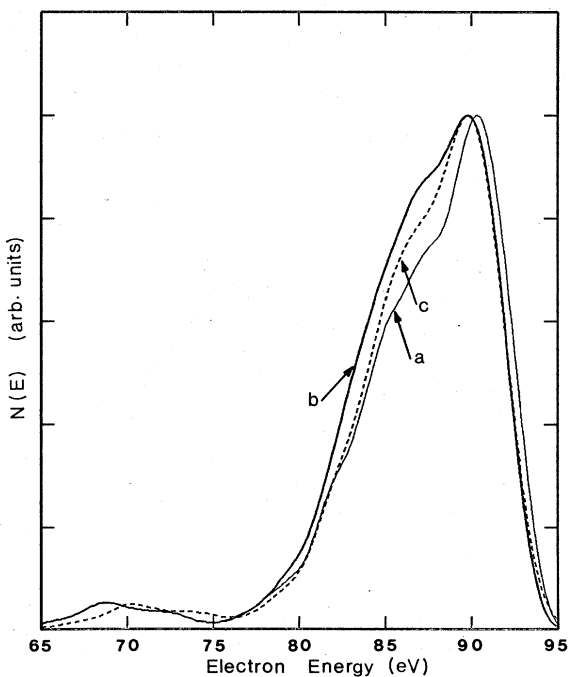


FIG. 5. Si L_{VV} Auger line shapes for atomic oxygen chemisorption. *a*—bulk line, *b*—effective Auger lines for chemisorbed surface (with no core-level shift), *c*—1.6-eV core-level shift.

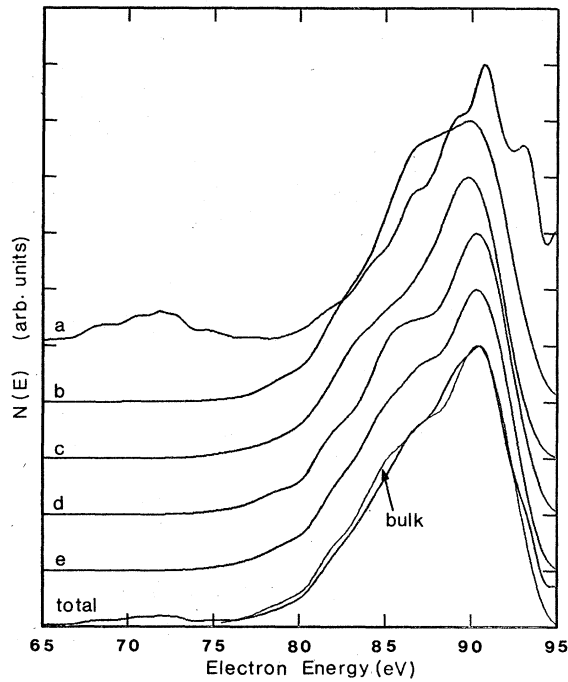


FIG. 6. The Si *LVV* Auger lines for the first five Si layers for molecular chemisorption. The effective line is compared with the Si bulk line.

match very closely with the bulk line, with an additional broad, weak peak centered around ~ 71 eV. Similar calculations were carried out for molecular chemisorbed oxygen with the first Si layer relaxed by 0.4 \AA . The effect of the Si-layer relaxation is to broaden the localized states. However these changes are not significant, and as expected the Auger line shapes remain more or less the same as for the unrelaxed case.

A model of the Si-SiO₂ interface has been discussed in paper I, in which an ordered interface is prepared by adjusting Si-O-Si bond lengths and angles to obtain perfect matching at the interface. The Si *LVV* Auger lines calculated for different layers are plotted in Fig. 7. The Auger lines show the corresponding features as seen in the density-of-states curves. The lines are referenced to the bulk Si *LVV* line. The main peak position appears shifted to the lower energy by 1.5 eV. Other prominent peak positions are 91, 85, 82.5, 79, 75, 71, and 69 eV. The effective Auger lines are also calculated applying the core-level shifts for the Si in SiO_x. The core-level shift for Si in SiO₂ is taken as 3.2 eV while that for the Si atoms at the interface is 1.6 eV. These shifts change the effective Auger line shape as shown in Fig. 8. A comparison of the line shapes shows that some of the fine

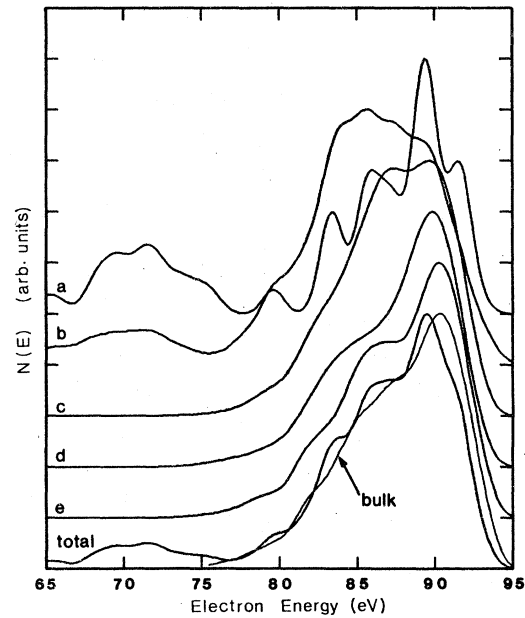


FIG. 7. The Si *LVV* Auger lines for various layers of the Si-SiO₂ interface. The model used for the interface is discussed in the text.

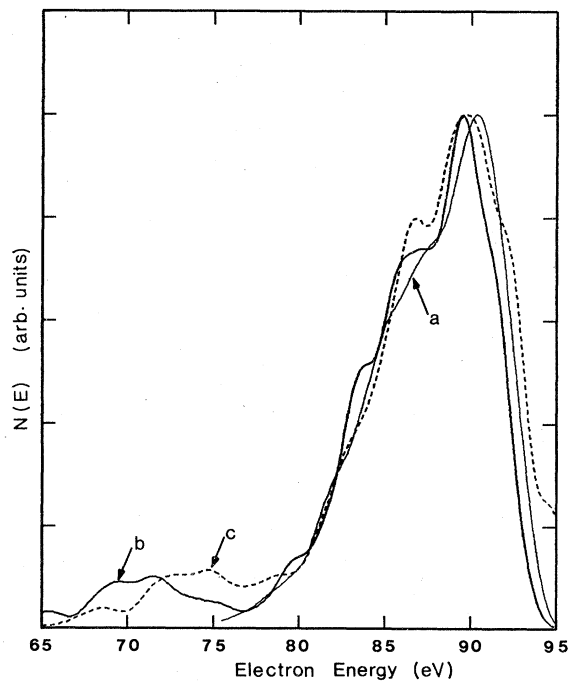


FIG. 8. Comparison of the Si *LVV* Auger line shapes for the interface; *a*—bulk lines; *b*—interface Auger line (zero core-level shift), and *c*—core-level-shifted Auger line.

structure is wiped out by the manner in which the different Auger lines from different layers overlap their contributions.

The calculations were repeated for a Si—O bond length of 1.55 Å. The overall features of the LDOS are also similar. However, the smaller bond length seems to reduce the density of states at -22 eV. Also, the characteristic peak at -4 eV is broadened at the peak itself and is slightly shifted to lower energy by 0.5 eV. The prominent peak at -2 eV for the Si in SiO₂ seems to split as well.

III. DISCUSSION

The silicon *LVV* Auger line shapes for the Si(100) surface with (i) a thin layer of oxide, (ii) chemisorbed molecular oxygen, (iii) atomic chemisorbed oxygen, and (iv) the Si bulk line are compared in Fig. 9. Each peak shows characteristic features which are summarized here. The molecular chemisorbed surface closely resembles the bulk line except for a broad peak centered around 71 eV. There are weak peaks around 85, 92, and 94.5 eV while the major peak is at ~ 90 eV. The major peak position in both atomic oxygen chemisorbed as well as oxide-formed surfaces are approximately 89 eV. At low-energy region, ~ 70 eV, both sur-

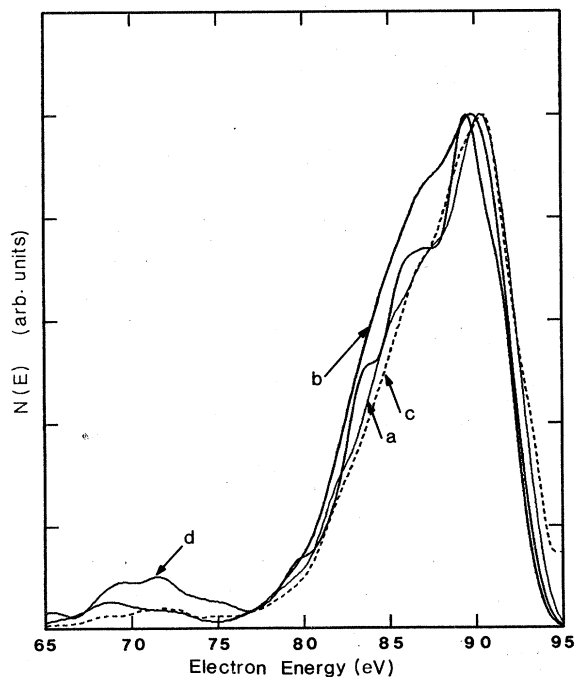


FIG. 9. Comparison of the Si *LVV* Auger line shapes *a*—bulk line, *b*—for atomic chemisorption, *c*—for molecular chemisorption, and *d*—for the interface.

faces give rise to small peaks which can be considered as characteristics of the Si—O bonds present. For the thin oxide interface, there are new states at 85, 83, 79, 75, 71, and 69 eV, whereas for the atomic oxygen chemisorbed surface there is a single peak at ~ 86 eV in addition to the low-energy peak at 70 eV. The atomic oxygen chemisorbed line is much broader than the other three line shapes.

In recent years, experimental studies of the Si-SiO₂ interface by Auger sputter profiling has revealed the presence of additional chemical states at the interface which are not attributable to either Si in SiO₂ or to bulk Si. Joyce and Neave¹⁵ in a study of the silicon-oxygen interaction using Auger electron spectroscopy noticed oxygen-induced states at 68 and 63 eV, a feature common to Si surfaces having an extensive coverage of oxygen. Garner *et al.*¹⁶ have observed additional structures at ~ 71 eV in the Si *LVV* transition for oxygen adsorbed on the Si(111) 2×1 surface. Helms *et al.*¹⁰ and Wager and Wilmsen¹⁷ observed a state in the Auger spectrum which has an energy about halfway between the peak of Si in SiO₂ and that of the free Si peak. This appears at ~ 83 eV compared to ~ 90 eV for bulk Si and ~ 74 eV for SiO₂. Morgen *et al.*¹⁸ observed similar states at a Si(111) surface during the adsorption of oxygen, in which peaks appear at 76.1, 73.1, 68.4, and 62.1 eV. Jost and Johnson¹⁹ observed an interface-related state around 83–85 eV. All of the above suggests the existence of additional chemical states attributable to the Si-SiO₂ interface. The results obtained here are similar to this experimental data. However, since many of these experiments are done for the Si(111) surface, a direct comparison of those numbers may not be appropriate, but many experimentalists suggest that the results of the (100) and (111) surfaces can be quite similar.

The results obtained here suggest that the initial oxidation of the Si(100) surface, as well as the characteristic Si-SiO₂ interface states in well-developed oxides, is primarily due to atomic oxygen bonded to the Si dangling orbitals. The LDOS obtained in paper I and the resulting Auger line shapes suggest that this is the more probable (rather than molecular chemisorption) result.

A final limitation to the results reported here should be mentioned. Throughout, we have assumed that the Si matrix elements remain the same as in bulk Si. These matrix elements reflect the local (atomic) environment and should therefore be affected by changes in the relative contributions of *s* and *p* wave functions to the bond charge. It can

therefore be expected that the matrix elements could change at the surface, or for different adsorbates, or for Si in SiO₂. Indeed, Jennison has recently shown this to be the case for Si in SiO₂.²⁰ Nevertheless, Feibelman and McGuire^{1,3} have shown that only minor corrections to the Auger line shape occur at the ideal Si(111) surface, and we hope for similar behavior here. Even if such changes in the bond charge occurred, they would predominantly produce small changes in the strength of partial DOS (matrix element changes) rather than in the positions of the dominant spec-

tra, and it is these positions that we are comparing to experiment. However, this limitation could be critical and without consistent matrix element calculations, such as those of Jennison,²⁰ the present results are only suggestive.

ACKNOWLEDGMENTS

The authors wish to express their appreciation for helpful discussions to C. W. Wilmsen, J. Wager, and B. T. Moore. This work was supported by the Office of Naval Research.

-
- ¹J. Feibelman and E. J. McGuire, *Phys. Rev. B* **17**, 690 (1978).
²R. Jennison, *Phys. Rev. B* **18**, 6865 (1978).
³P. J. Feibelman, E. J. McGuire, and K. C. Pandey, *Phys. Rev. B* **15**, 2202 (1977).
⁴J. E. Houston, G. Moore, and M. G. Lagally, *Solid State Commun.* **21**, 879 (1977).
⁵D. E. Ramaker, J. S. Murday, N. H. Turner, G. Moore, M. G. Lagally, and J. Houston, *Phys. Rev. B* **19**, 5375 (1979).
⁶D. E. Ramaker and J. S. Murday, *J. Vac. Sci. Technol.* **16**, 510 (1979).
⁷D. R. Jennison, *Phys. Rev. Lett.* **40**, 807 (1978).
⁸J. A. D. Mathew and Y. Kominos, *Surf. Sci.* **53**, 716 (1975).
⁹M. L. Tareg and G. K. Wehner, *J. Appl. Phys.* **44**, 1534 (1973).
¹⁰C. R. Helms, Y. E. Strausser, and W. E. Spicer, *Appl. Phys. Lett.* **33**, 767 (1978).
¹¹J. S. Johannessen and W. E. Spicer, *J. Appl. Phys.* **47**, 3028 (1976).
¹²J. T. Grant, R. G. Wolfe, M. P. Hooker, R. W. Springer, and T. W. Hass, *J. Vac. Sci. Technol.* **14**, 232 (1977).
¹³T. Kunjunny and D. K. Ferry, preceding paper, *Phys. Rev. B* **24**, 4593 (1981).
¹⁴A. Ishazaka and S. Iwata, *Appl. Phys. Lett.* **36**, 71 (1980).
¹⁵B. A. Joyce and J. H. Neave, *Surf. Sci.* **27**, 499 (1971).
¹⁶C. M. Garner, I. Lindau, C. Y. Yu, P. Pianetta, J. N. Miller, and W. E. Spicer, *Phys. Rev. Lett.* **40**, 403 (1978).
¹⁷J. F. Wager and C. W. Wilmsen, *J. Appl. Phys.* **50**, 874 (1979).
¹⁸P. Morgen, J. H. Onsgaard, and S. Tongaard, *Appl. Phys. Lett.* **34**, 488 (1979).
¹⁹S. R. Jost and W. C. Johnson, *Appl. Phys. Lett.* **36**, 446 (1980).
²⁰D. R. Jennison, *Bull. Am. Phys. Soc.* **26**, 220 (1981).